Journal of
Water & Climate Change

IWA PUBLISHING

Journal of Water and Climate Change Vol 14 No 11, 4068 doi: 10.2166/wcc.2023.260

Unraveling the dynamics of climate: empirical evidence from the Indian state of West Bengal

Soumik Das * and Kishor Goswami

Department of Humanities and Social Sciences, Indian Institute of Technology Kharagpur, West Bengal, India, PIN-721302
*Corresponding author. E-mail: pallab.iam@iitkgp.ac.in

SD, 0000-0003-2552-2043; KG, 0000-0002-9489-6826

ABSTRACT

Understanding climate variability and trends is crucial for managing a host of sectors. Everything from water availability to agricultural productivity is affected by variability and trends in temperature, rainfall, evapotranspiration, and solar radiation. Nevertheless, their dynamics have seldom been explored together, especially in India. To address this gap, the present study investigates the variability, trend, and magnitude of those parameters individually and concurrently using fractal dimension and non-parametric statistics over the Indian state of West Bengal from 1951 to 2020. The results show a south–north gradient in overall climate variability. The Gangetic West Bengal (GWB) is experiencing higher variability, along with a rising minimum temperature ($\geq$0.008 °C year^{-1}) and declining rainfall ($\geq -$ 1 mm year^{-1}). Though the Sub-Himalayan West Bengal as a whole shows less variability, its foothills reveal modest variation coupled with increasing maximum temperature ($\geq$0.005 °C year^{-1}), reference evapotranspiration ($\geq$0.4 mm year^{-1}), and decreasing rainfall in the post-monsoon and winter seasons. Based on the results, we identified the western GWB, the Sundarbans, and the sub-Himalayan foothills as the most vulnerable areas and recommended proactive crop and water management strategies. Finally, we underline the need to analyze climate dynamics holistically to manage climate-sensitive sectors efficiently and sustainably.

Key words: climate dynamics, fractal dimension, Mann–Kendall, trend, variability, West Bengal

HIGHLIGHTS

- Analyzed the variability, trend, and magnitudes of five critical climatic parameters.
- The variability of climate dynamics shows a south–north gradient.
- The western, coastal, and foothill regions exhibit a complex and uncertain climate.
- The results are discussed in terms of their possible impacts on agricultural and water resources.

GRAPHICAL ABSTRACT

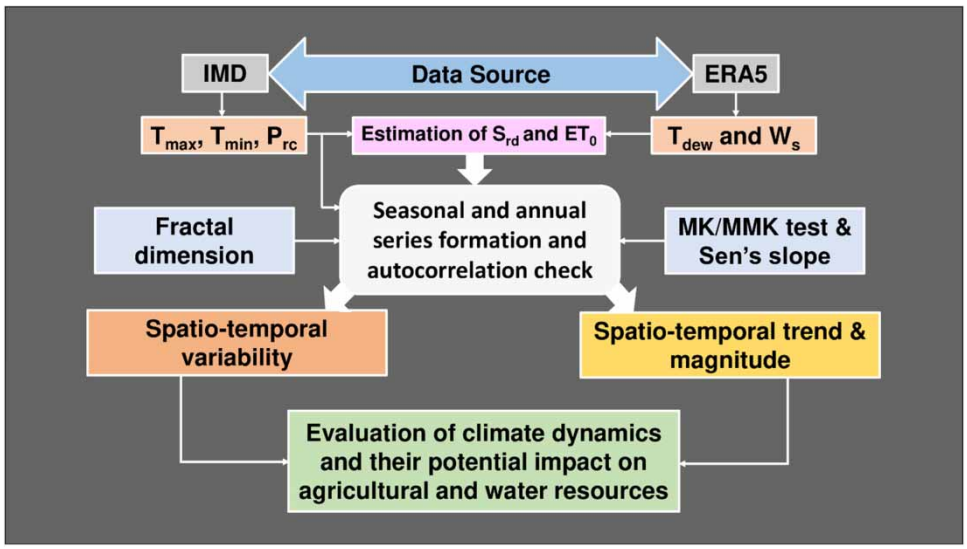

1. INTRODUCTION

In general, scientists agree that anthropogenic activities substantially raise the concentration of greenhouse gases (GHGs) and trigger large-scale variations in atmospheric processes (Ramanathan *et al.* 2007). This enhanced rise in GHGs alters the Earth's overall climatic condition through changes in different climatic parameters. Thus, assessing the nature, variability, and trend of critical climatic parameters holds significant importance not only for understanding the environmental state but also for managing climate-induced sectors such as water, agriculture, biodiversity, and ecosystem services (Rao *et al.* 2015; Srivastava *et al.* 2016; Xu *et al.* 2017). Such information also serves as a basis for formulating sector-specific climate-resilient strategies.

In order to combat climatic adversities, researchers around the world have urged a holistic evaluation of climate change (Kim & Ivanov 2015; Boyd 2017), which necessitates a more in-depth and holistic approach. Even after the growing call, emphasis has mostly been given to maximum temperature (T_{max}), minimum temperature (T_{min}), and rainfall (P_{rc}). Consequently, other parameters, like solar radiation (S_{rd}) and reference evapotranspiration (ET_0), which are crucial and have significant contributions in agriculture to human health, remain less explored. Furthermore, most research focused on monotonic trends (for instance, Dash *et al.* 2007; Bandyopadhyay *et al.* 2009; Jhajharia *et al.* 2012; Sonali & Kumar 2013; Rao *et al.* 2014; Rao *et al.* 2015; Mukhopadhyay *et al.* 2016; Sharma *et al.* 2016; Basha *et al.* 2017; Datta & Das 2019a, 2019b; Das *et al.* 2022; Mann & Gupta 2022) while trivializing overall or holistic climate variability. Since the climate is chaotic with high variabilities (Rind 1999; Xu *et al.* 2016), such ignorance may have a detrimental impact on many sectors, especially in agriculture and water resources.

Besides other parameters, the primary driving factors of field-crop production (such as water availability, soil moisture content, and the duration and intensity of sunlight) are explicitly controlled by T_{max}, T_{min}, P_{rc}, ET_0, and S_{rd} variability (Cline 2008; Rao *et al.* 2014; Jabal *et al.* 2022). Undeniably, climate change has substantially affected almost all sectors that drive human life and livelihoods. However, the impact on agriculture is widespread and alarming (Das & Goswami 2021), where studies have shown that it would reduce crop yield to a great extent, even after accounting for the benefits of CO_2 fertilization on crop growth (Parry *et al.* 2004; Rao *et al.* 2015). A rapid and unprecedented alteration in climatic patterns may have cascading effects, beginning with a dip in agricultural production and escalating through food security, employment, and, eventually, the economy of the nation. Several climate-induced hazardous events have occurred in India during the last two decades, wreaking havoc on the agricultural economy. The estimated revenue loss from such impact ranges between 15 and 18% (Government of India 2018a). Therefore, it is essential to analyze climate dynamics holistically in a country like India, where agriculture contributes to 16.38% of the country's gross domestic product (MOSPI 2021), employs over 60% of the population (Srivastava *et al.* 2016), and feeds more than 17% of the world's population (Singh *et al.* 2014).

While a large-scale assessment of climate dynamics is essential to comprehend the larger picture, regional-level studies may be more significant for policy implementation. In light of this, we choose the Indian state of West Bengal as a study site. West Bengal is India's only state that extends from the mighty Himalayas in the north to the Bay of Bengal in the south, with diverse physiographic, climatic, and agricultural conditions. Such diversities make this state suitable for analyzing spatio-temporal variability and trends in climatic parameters and could adequately reflect the national situation. Also, the state's economy relies on the climate-sensitive agricultural sector, and issues related to inconsistent rainfall, rising temperature, floods, drought, cyclones, and pests and diseases (Datta & Das 2019a) have become a common phenomenon. For instance, in 2008–09, the yield of Boro[1] rice dropped by 14% due to the scorching summer, resulting in an 11.5% fall in overall Boro rice production (Government of West Bengal 2010).

Given this context, the present study intends to explore (i) the spatial variability of climate dynamics at seasonal and annual scales by using fractal dimension theory and (ii) the spatio-temporal trend and magnitudes in key meteorological parameters (T_{max}, T_{min}, P_{rc}, ET_0, and S_{rd}) throughout West Bengal by employing multiple non-parametric statistics. Moreover, this is a first-of-its-kind variability and trend assessment in the Indian context by integrating five crucial climatic variables: T_{max}, T_{min}, P_{rc}, ET_0, and S_{rd}. Such a combined study, comprising both variability and trend, is expected to provide a more holistic understanding of the changing climate dynamics and their potential implications for agriculture and water resources in West Bengal. Moreover, this approach could unravel more detailed features of climate change than an independent assessment of a single or pair of climatic factors. The resultant variability, trend, and magnitude of those critical climatic parameters would provide a basis for policymakers to craft suitable adaptation strategies for effectively managing agricultural and water resources to attain sustainable food security.

2. MATERIALS AND METHODS

2.1. The study area

With an area of 88,752 km^2, West Bengal is the 14th largest state in India and makes up around 2.7% of the country's total land area. As per the Census of India (2011), the state has 19 districts (Figure 1(a)). The state falls into three broad climatic classes: Cwb[2], Cwa[3], and Aw[4] as delineated by Peel *et al.* (2007). Rainfall is the primary water source, and most of it falls during the monsoon season, which begins in the first week of June and ends within a fortnight of October.

The India Meteorological Department (IMD) has bifurcated the entire state into two distinct sub-divisions: Gangetic West Bengal (GWB) and Sub-Himalayan West Bengal (SHWB). Generally, the latter receives more rainfall than the former due to the northward shift of the monsoon trough (IMD 2008) and its vicinity to the Himalayan range (Figure 1(b)). During the pre-monsoon season (March–May), sporadic rainfall occurs throughout the state due to Nor'wester thunderstorms (Sadhukhan *et al.* 2000). In contrast, the post-monsoon season (October–November) frequently witnesses tropical cyclones, particularly along the coast (Datta & Das 2019a). The winter, on the other hand, is rather dry and cold. During summer, the western parts of GWB frequently encounter heatwaves, with T_{max} exceeding 45 °C (IMD 2008; Datta & Das 2019a). The northernmost districts rarely experience extreme temperatures, while the hilly areas of the Darjeeling district get occasional winter snowfalls. The Bauxa region (in the foothills of SHWB) receives the highest rainfall, while Purulia (in western GWB) the least in West Bengal.

2.2. Data type and source

The daily gridded time series of rainfall and temperature (both the T_{max} and T_{min}) data covering a period of 70 years (from 1951 to 2020) were acquired from the IMD's official web portal (https://www.imdpune.gov.in/Clim_Pred_LRF_New/Grided_Data_Download.html). The high-resolution gridded rainfall (0.25° × 0.25°) data were developed using observations from over 6,995 gauge stations spread across India (Pai *et al.* 2014), whereas gridded temperature (1° × 1°) data were created using observations from 395 quality-controlled stations (Srivastava *et al.* 2009). On the other hand, the high-resolution (0.25° × 0.25°) wind speed (at 10 m height) and dew point temperature data covering the same period (1951–2020) were obtained from the ERA5 atmospheric reanalysis products (Hersbach *et al.* 2020) developed by the European Centre for

[1] A wet variety of paddy sown in winter and harvested in summer.

[2] C: Temperate; w: Dry winter; b: Warm summer.

[3] C: Temperate; w: Dry winter; a: Hot summer.

[4] A: Tropical; w: Savannah.

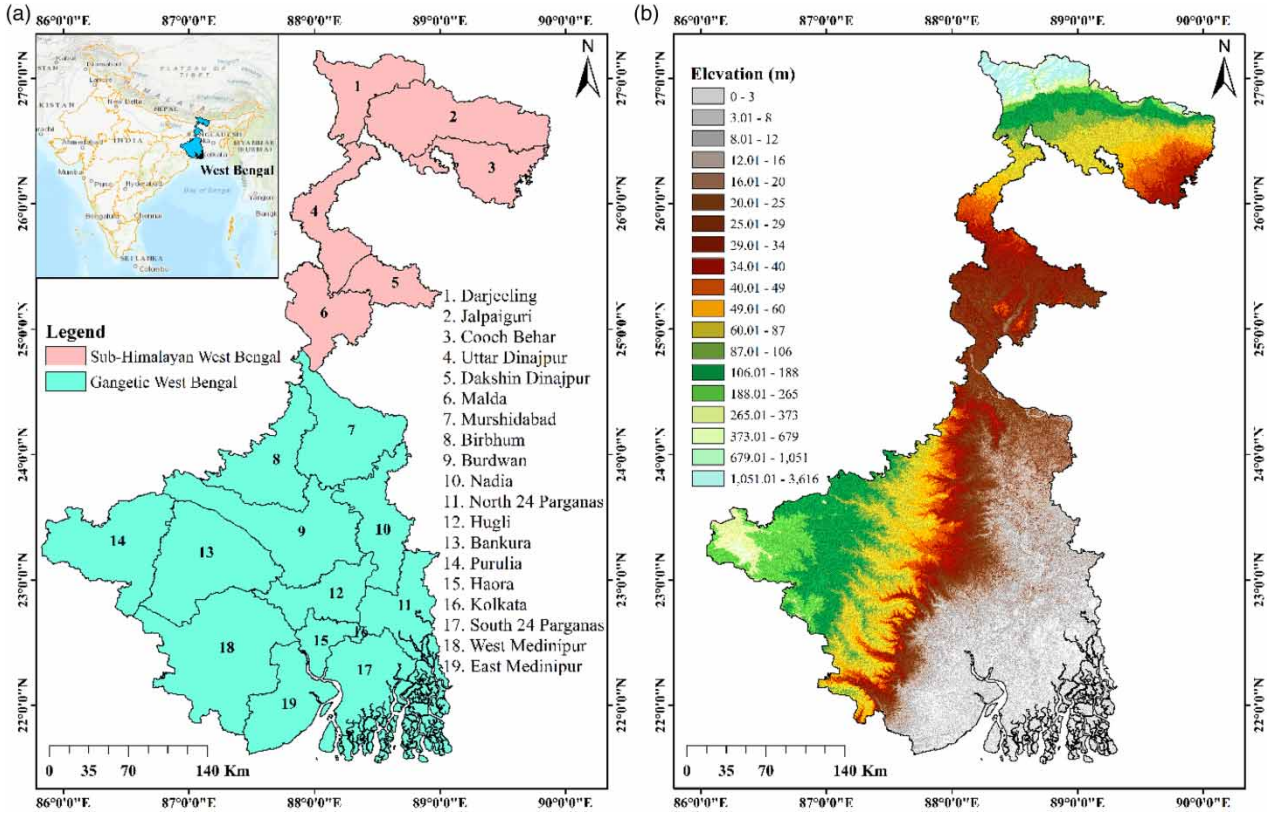

Figure 1 | Location of the study area showing (a) districts of West Bengal (obtained from http://www.diva-gis.org/gdata) along with meteorological sub-divisions and (b) elevation map (generated from the Digital Elevation Model of Shuttle Radar Topography Mission, obtained from https://earthexplorer.usgs.gov/).

Medium-Range Weather Forecasts (ECMWF). The ERA5 products were chosen in this study because of their improved horizontal and vertical resolutions, bias correction, and analysis based on a 10-member ensemble 4D-Var (Mahto & Mishra 2019).

2.3. Methods

2.3.1. Data pre-processing

In order to ensure consistency and comparability with other products, the coarse temperature data were resampled to 0.25° × 0.25° spatial resolution using a bi-linear interpolation technique. The S_{rd} was computed from the air temperature differences using the Hargreaves–Samani radiation formula (Hargreaves & Samani 1985), which is expressed as

$$R_s = K_{Rs}\sqrt{(T_{max} - T_{min})}.R_a \quad (1)$$

where R_s is the solar radiation (MJ m^{-2} day^{-1}), T_{max} and T_{min} are the maximum and minimum air temperature (°C), and K_{Rs} represent empirically adjusted coefficients in which 0.16 and 0.19 were set for interior and coastal regions, respectively. R_a is the extraterrestrial radiation (MJ m^{-2} day^{-1}), estimated using Equation (2).

$$R_a = \frac{24 \times 60}{\pi} \times G_{sc}.d_r[\omega_s sin(\phi)sin(\delta) + cos(\delta)cos(\delta)sin(\omega_s)] \quad (2)$$

where G_{sc} is the solar constant, i.e., 0.0820 (MJ m^{-2} min^{-1}), d_r is the Earth–Sun inverse relative distance, ω_s is the sunset hour angle (rad), ϕ is the station latitude (rad), and δ is the solar declination (rad). The values of d_r, ω_s, ϕ, and δ were calculated using the methods of Allen *et al.* (1998). The acquired wind speed (U_2) data were at 10 m height, which we transformed into the

required height (2 m) using Equation (3) as suggested by Allen *et al.* (1998).

$$U_2 = U_z \frac{4.87}{\ln(67.8z - 5.42)} \tag{3}$$

where U_2 is the wind speed at 2 m height, U_z is the measured wind speed at z_m above the ground surface (m s^{-1}), and z is the elevation of the grid point above sea level (m).

2.3.2. Estimation of reference evapotranspiration (ET_0)

In the present study, the FAO-56 PM method (Allen *et al.* 1998) was applied, which is well-recognized and considered the standard model for estimating ET_0 and is expressed as

$$ET_0 = \frac{0.408\Delta(R_n - G) + \gamma(900/(T + 273))U_2(e_s - e_a)}{\Delta + \gamma(1 + 0.34U_2)} \tag{4}$$

where ET_0 is the reference evapotranspiration (mm day^{-1}), R_n is the net radiation at crop surface (MJ m^{-2} day^{-1}), G is the soil heat flux density (MJ m^{-2} day^{-1}), T is the average daily air temperature at 2 m height (°C), U_2 is the wind speed at 2 m height (m s^{-1}), e_s is the saturation vapor pressure (kPa), e_a is the actual vapor pressure (kPa), $e_s - e_a$ is the saturation vapor pressure deficit (kPa), Δ is the slope of the vapor pressure curve (kPa °C^{-1}), and γ is the psychometric constant (kPa °C^{-1}). The soil heat flux (G) is considered 0, as the degree of daily G underneath the grass reference surface is relatively small and, therefore, ignored (Allen *et al.* 1998). The net radiation (R_n) was estimated using the following equations (Equations (5)–(9)).

$$R_{nl} = (R_{ns} - R_{nl}) \tag{5}$$

$$R_{ns} = (1 - \alpha)R_s \tag{6}$$

$$R_{so} = (a_s + b_s)R_a \tag{7}$$

where R_{ns} is the net shortwave radiation (MJ m^{-2} day^{-1}), α is the albedo or canopy reflection coefficient, R_s is the solar radiation (MJ m^{-2} day^{-1}), and R_{so} is the clear-sky radiation (MJ m^{-2} day^{-1}). In this study, the coefficients $\alpha = 0.23$, $a_s = 0.25$, and $b_s = 0.50$ were used as recommended in the FAO-56 paper (Allen *et al.* 1998). The net outgoing longwave radiation (MJ m^{-2} day^{-1}), R_{nl}, was estimated as

$$R_{nl} = \sigma\left(\frac{T_{max,K}^4 + T_{min,K}^4}{2}\right)(0.34 - 0.14\sqrt{e_a})\left(1.35\frac{R_s}{R_{so}} - 0.35\right) \tag{8}$$

$$e_a = 0.6108exp\left[\frac{17.27T_{dew}}{T_{dew} + 237.3}\right] \tag{9}$$

$$e_s = \frac{0.6108exp(17.27T_{max}/(T_{max} + 237.3)) + 0.6108exp(17.27T_{min}/(T_{mib} + 237.3))}{2} \tag{10}$$

where e_s is the mean saturation vapor pressure (kPa), e_a is the actual vapor pressure function (kPa), T_{max} and T_{min} are the maximum and minimum air temperature (°C), respectively, and *exp* [..] is 2.7183 (base of natural logarithm) raised to the power [..]. σ represents the Stefan–Boltzmann constant (4.903×10^{-9} MJ K^{-4} m^{-2} day^{-1}), $T_{max,K}$ and $T_{min,K}$ are the maximum and minimum absolute temperature during the 24 h (K), respectively, and T_{dew} is the dew point temperature at 2 m height. The vapor pressure curve (Δ) slope and psychometric constant (γ) were calculated using the following Equations

(11)–(13), respectively:

$$\Delta = \frac{4098[0.6108exp(17.27T_{avg}/(T_{avg}+237.3))]}{(T_{avg}+237.3)^2} \tag{11}$$

$$\gamma = \frac{C_p P}{\varepsilon \lambda} = 0.665 \times 10^{-3} P \tag{12}$$

$$P = 101.3\left(\frac{293 - 0.0065Z}{293}\right)^{5.26} \tag{13}$$

where T_{avg} is the mean air temperature (°C), P is the atmospheric pressure (kPa), λ is the latent heat of vaporization, i.e., 2.45 (MJ kg^{-1}), C_p is the specific heat at constant pressure, i.e., 1.013×10^{-3} (MJ kg^{-1} °C^{-1}), and ε is the ratio molecular weight of water vapor/dry air, i.e., 0.622.

2.3.3. Formulation of seasonal and annual data

Only the grids falling inside the state of West Bengal were considered to analyze the variability, trend, and magnitude. The gridded daily data were then transformed into annual and seasonal scales using the conventional summation (for P_{rc} and ET_0) and average (for T_{max}, T_{min}, and S_{rd}) techniques, with four dominant seasons as defined by Rathore *et al.* (2013): pre-monsoon (March–May), monsoon (June–September), post-monsoon (October–November), and winter (December–February). The study includes annual and seasonal series as the variability and trends, manifesting not only on an annual scale but also in its distinct seasons. Furthermore, a statistically significant (upward) trend on an annual scale may reflect a non-significant (downward) pattern on seasonal scales.

2.3.4. Computation of fractal dimensions

The fractal dimension unravels complex features from geophysical time series, viz., variability, persistency, and self-similarity, and is extensively used across many disciplines (Rangarajan & Sant 2004; Cui *et al.* 2022). It enables mimicking a given period's variational properties to a period with significantly finer temporal resolution (Fortuna *et al.* 2014; Xu *et al.* 2017). Since the climate system displays such comparable features over different temporal scales, using fractal theory to investigate the variability may better comprehend the climate dynamics spanning from seasonal to annual scales. In recent times, the fractal dimension (D) has been applied through the Hurst Index (HI) to study the long-term variabilities of climate (Rangarajan & Sant 2004; Xu *et al.* 2017). The HI of climate time series can be obtained from the rescaled range analysis (R/S) as recommended by Hurst (1951) and evolved into a fractal theory for analyzing complex properties of time series by Mandelbrot & Wallis (1969). The basic principle to compute the HI from R/S is as follows. For a particular climatic variable's time series, say, $t = 1, 2 \ldots n$, $x(t)$, the value of that climatic variable at time t and the mean sequence x_μ for any integer μ is defined as

$$x_\mu = \frac{1}{\mu}\sum_{t=1}^{\mu} x(t), \quad \text{where } \mu = 1, 2 \ldots n \tag{14}$$

Therefore, the cumulative deviation $X(t, \mu)$ is

$$X(t, \mu) = \sum_{u=1}^{t} [x(u) - x_\mu], \ 1 \le t \le \mu \tag{15}$$

The range sequence $R(\mu)$ can be obtained from Equation (16), as expressed below.

$$R(\mu) = \{\max X(t, \mu)\} - \{\min X(t, \mu)\}, \quad \text{where } t = 1, 2 \ldots n \tag{16}$$

The range is then divided by the standard deviation, $S(\mu)$, which is expressed as follows:

$$S(\mu) = \sqrt{\frac{1}{\mu}\sum_{t=1}^{\mu}[x(t) - x_{\mu}]^2} \tag{17}$$

The standardization enables comparison between various events and timeframes. Hurst (1951) discovered that the rescaled range, $R/S = R(\mu)/S(\mu)$, can accurately be established by the following relationship.

$$\frac{R}{S} = (\alpha\mu)^H \tag{18}$$

where α is a constant and H is the Hurst exponent. In order to achieve the linear relationship between the R/S and μ, a log transformation to Equation (18) is then applied. As a result, H becomes the only linear coefficient and can be computed using the least squares method (Xu *et al.* 2017). Following this process, one can easily obtain any climatic parameter's fractal dimension (D). The relationship between D and H was established by Feder (1988) and can be expressed as follows:

$$D = (2 - H) \tag{19}$$

The D value varies from 1 to 2. When D is 1.5, there is no correlation between the magnitude changes corresponding to the two successive timeframes, indicating complete randomness. As a result, neutral or no pattern can be discerned from that particular data, which leads to a highly uncertain process (Rangarajan & Sant 2004). However, a positive correlation can be observed if the D value is between 1 and 1.5, suggesting that a rise in the magnitude of the preceding data is likely to persist in the following data. As the fractal dimension decreases to 1, the process becomes more and more predictable as it exhibits a persistent character (Cui *et al.* 2022). A negative correlation, on the other hand, may be inferred when D increases from 1.5 to 2, indicating that the variable under consideration is most likely to decline in the event of an increase in the amplitude of the previous data. Therefore, the time series displays anti-persistency when the fractal dimension value is close to 2 (Harrouni & Guessoum 2009). The higher the value of D of a climatic parameter the greater its variability, signifying that the climatic variables under investigation change with more frequency and uncertainty and vice versa (Xu *et al.* 2017). In this study, following Xu *et al.* (2017), we defined climate dynamics as a multiplication of the D values of those five meteorological parameters (since the considered variables interact conjointly at the same time) and computed it at seasonal and annual scales.

2.4. Identification of trends and their magnitudes

The non-parametric Mann–Kendall (MK) test (Mann 1945; Kendall 1975) was applied to examine trends in the long-term climatic parameters. The MK test is appropriate as the data need not pursue a specific distribution. However, significant positive autocorrelation in the data can augment the likelihood of trends while there is no trend, and *vice versa* (Hamed & Rao 1998). Therefore, the variance correction approach, namely the Modified Mann–Kendall (MMK) test suggested by Hamed & Rao (1998), was applied to eliminate the effect of autocorrelation from the time series. The magnitude of the obtained trend was computed by non-parametric Sen's slope estimator (SSE) (Sen 1968). All the statistical significance was measured at a 95% confidence interval, i.e., $\alpha = 0.05$. The mathematical formulas of MK/MMK and Sen's slope were presented in Supplementary material, Methods S1–S3.

Data pre-processing, curation, and analysis were performed in CDO (version 1.9.9) and RStudio (version 4.1.1), while the necessary maps were generated using the ArcGIS software (version 10.4.1). Figure 2 illustrates the entire methodological procedure followed in the present study.

3. RESULTS

3.1. Spatio-temporal variability in climate dynamics

The spatial pattern of seasonal and annual variability in climate dynamics is shown in Figure 3. The western and southwestern GWB (Purulia, Bankura, and West Medinipur districts) showed high seasonal and annual variability. However, the whole SHWB region showed less variability in climate dynamics, albeit some patches in the far north and northeastern side (Darjeeling, Jalpaiguri, and Cooch Behar districts) revealing a modest degree of variability during the pre-monsoon and winter

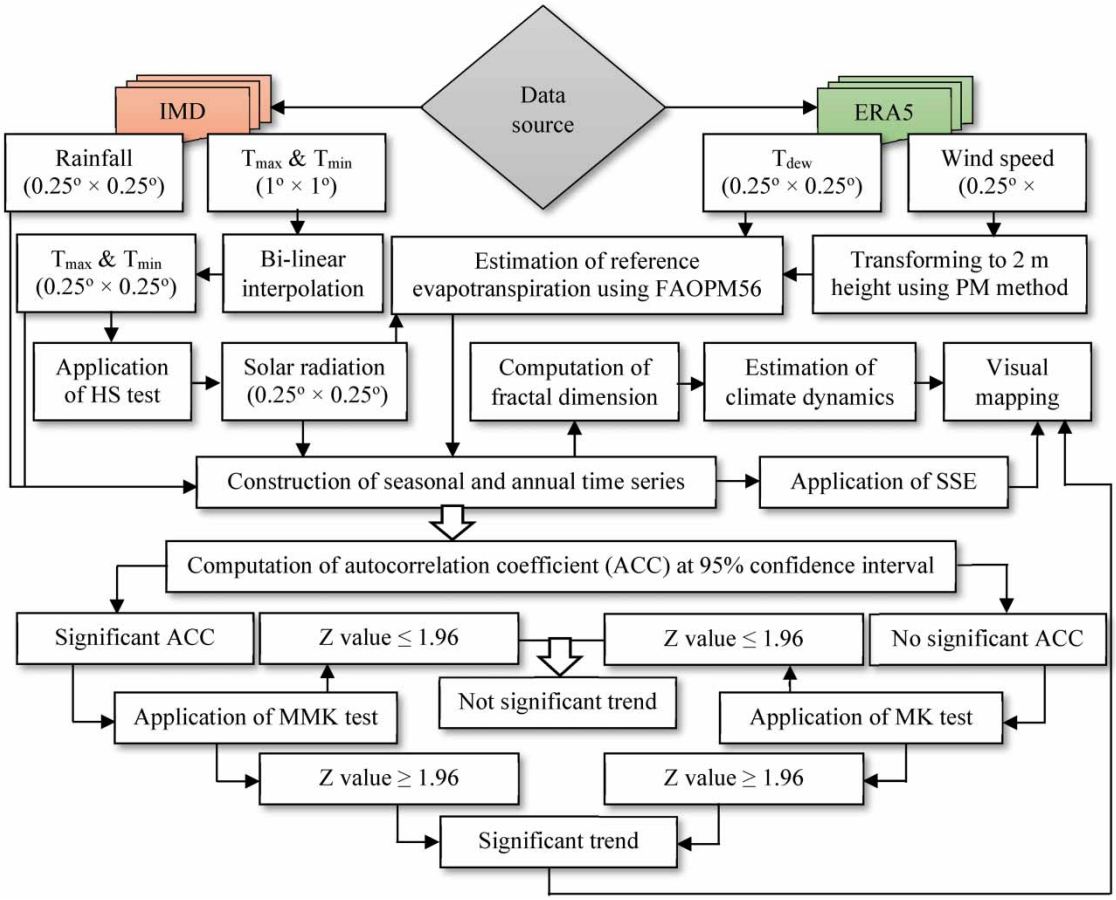

Figure 2 | Methodological flowchart of the study.

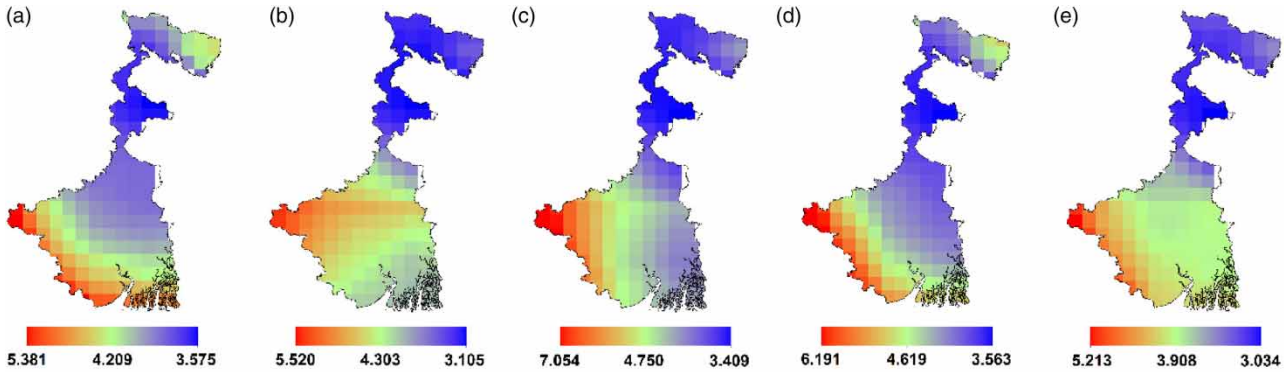

Figure 3 | Spatial variability of climate dynamics during (a) pre-monsoon, (b) monsoon, (c) post-monsoon, (d) winter, and (e) annual scale in West Bengal from 1951 to 2020. The legend represents fractal dimension values, deciphering the variability. Higher fractal dimension signifies greater degree of variability.

seasons. The western GWB (Purulia district) and the southern SHWB (specifically Malda and Dakshin Dinajpur districts) exhibit the highest (7.054) and lowest (3.034) variability in climate dynamics at the post-monsoon and annual scales, respectively.

Considering the T_{max} (Supplementary Figure S1), higher variabilities with a fractal dimension ranging from 1.472 to 1.548 were primarily observed in the northern SHWB and southern GWB during pre-monsoon and winter and western and south-western GWB during monsoon and post-monsoon seasons. The southern and southeastern GWB witnessed a neutral pattern

(as the D value reaches 1.500) on the annual scale. Regarding T_{min} (Supplementary Figure S2), most of the central and western parts of the GWB showed a high level of variability (1.288–1.519), whereas the entire SHWB showed lesser variability (1.210–1.306) irrespective of seasonal or annual timescales. It is noticed that areas with higher variability gradually diminished with the passage of seasons (pre-monsoon to winter).

We observed quite a homogeneous spatial variability of P_{rc}, i.e., no substantial differences throughout the seasons, including annual scales (Supplementary Figure S3). The variabilities gradually decreased from 1.516 in the western and southwestern GWB (Purulia, East Medinipur, and West Medinipur districts) to 1.210 in the northernmost SHWB (Darjeeling Himalayas).

As for ET_0 (Supplementary Figure S4), the western and southwestern parts (Purulia, East Medinipur, and West Medinipur districts) and some patches over coastal GWB (South 24 Parganas district) exhibited consistently higher variability (1.398–1.486). In contrast, the central and southern SHWB (especially in Malda, Dakshin Dinajpur, and Uttar Dinajpur districts) revealed lesser variability (1.238–1.298) throughout the seasonal and annual timescales. Except for the monsoon, several grids in northern and northeastern SHWB (Darjeeling, Jalpaiguri, and Cooch Behar districts) and eastern GWB (Nadia, North 24 Parganas, Howrah, Kolkata, Eastern Burdwan, and some portion of Murshidabad) displayed high and low variability across seasonal and annual scales, respectively.

Concerning the S_{rd} dynamics (Supplementary Figure S5), the whole SHWB showed fractal dimensions lower than 1.250, except for a few grids in the northeastern section, which were only present during the pre-monsoon and winter seasons. However, the western and southwestern areas of the GWB (e.g., the western part of Purulia, East Medinipur, and West Medinipur districts) revealed higher fractal dimensions ranging from 1.384 to 1.434, indicating the strongest variability (Supplementary Figure S5c).

Upon examining the variability of the studied parameters individually (Supplementary Figures S1–S5), it is found that the temperature (both T_{max} and T_{min}) had the highest variability, followed by ET_0, while P_{rc} and S_{rd} had the lowest variability, irrespective of seasonal and annual scales. Barring a few grids from T_{max} and T_{min}, the fractal dimensions of the considered climatic parameters revealed a mostly persistent nature, indicating that the future trend may likely follow the present pattern. The anti-persistent nature is mainly witnessed in pre-monsoon, winter, and post-monsoon seasons of the T_{max}, T_{min}, and P_{rc} parameters, translating that a decrease (increase) in the degree of variability is more likely to follow an increasing (decreasing) pattern in the near future. Quite a few grids, on the other hand, particularly from T_{max} (during pre-monsoon) and T_{min} (during post-monsoon), showed a fractal value of exactly 1.5, i.e., complete randomness in the data, leading to a highly uncertain process and thus unpredictable. The fractal dimension of the studied parameters ranges between 1.210 and 1.548, confirming the self-affine characteristics, i.e., repeating patterns across scales. It was evident in the spatio-temporal variability of climate dynamics (Figure 3), including the individual variability of the studied climatic variables (Supplementary Figures S1–S5). For instance, the variability of climate dynamics (Figure 3) is almost identical during the pre-monsoon and winter seasons. Likewise, the variability of monsoon dynamics exhibited repetitive behavior on the annual scale.

3.2. Climate trends and their magnitudes

With varying significance, the T_{max} increased consistently in SHWB throughout the seasonal and annual timeframes (Figure 4). The foothill region of the SHWB (Darjeeling, Jalpaiguri, and Cooch Behar districts) along with the southernmost GWB (including the entire coastal Sundarbans, the southern part of East Medinipur, and West Medinipur districts) showed no significant increasing trends at a magnitude of 0.001 °C year^{-1}. In contrast, the rest of the areas (i.e., the eastern, western, and central GWB and the southern and central SHWB) showed significant decreasing trends at a magnitude of 0.009–0.018 °C year^{-1}. The monsoon and post-monsoon seasons (Figure 4(b) and 4(c)) had a north–south trend difference with an almost identical pattern of statistical significance. The only noticeable difference is that the north–south trend contrast was more prominent in the monsoon season than in the post-monsoon. In the post-monsoon season, some isolated grids with minimal trend magnitude were discovered in the northern kin, which was absent during the monsoon season. Like monsoon and post-monsoon, a similar spatial pattern of T_{max} was observed during winter and annual scales (Figure 4(d) and 4(e)), but with different nature, magnitude, and statistical significance.

The magnitude of T_{min} revealed both increasing and decreasing trends throughout West Bengal (Figure 5). However, we did not find much statistical significance across seasonal and annual scales, except for a few grids in the monsoon and post-monsoon seasons. The entire SHWB, including the eastern parts of the GWB region, showed a rising pattern during pre-monsoon and monsoon seasons (Figure 5(a) and 5(b)). Then, the trend faded and concentrated on the central and eastern

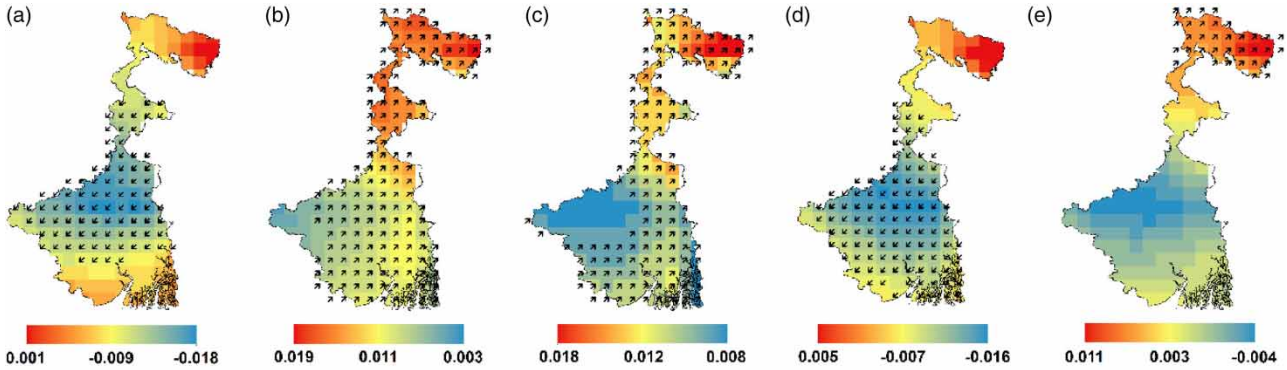

Figure 4 | Spatial trend and magnitude in maximum temperature (°C year^{-1}) during (a) pre-monsoon, (b) monsoon, (c) post-monsoon, (d) winter, and (e) annual scale in West Bengal from 1951 to 2020. The tilted upward arrows indicate significant ($\alpha = 0.05$) increasing trend and *vice versa*.

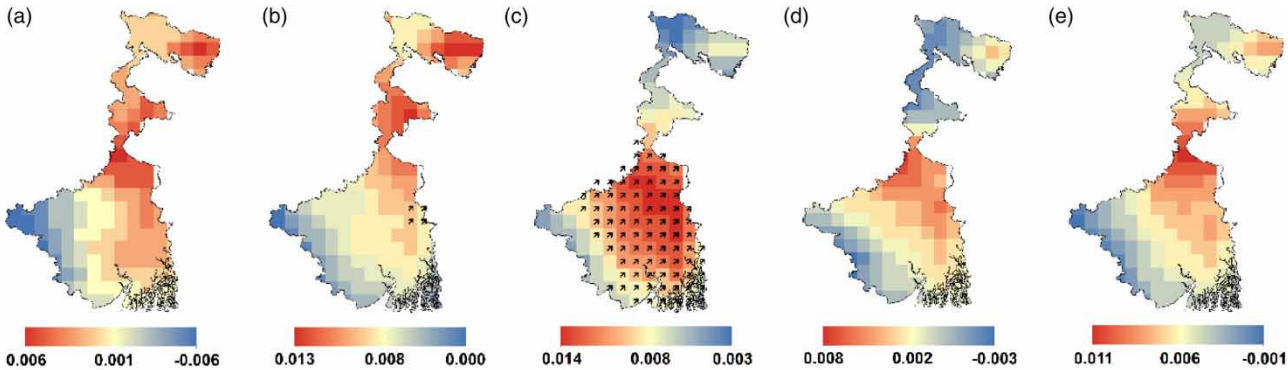

Figure 5 | Spatial trend and magnitude in minimum temperature (°C year^{-1}) during (a) pre-monsoon, (b) monsoon, (c) post-monsoon, (d) winter, and (e) annual scale in West Bengal from 1951 to 2020. The tilted upward arrows indicate significant ($\alpha = 0.05$) increasing trend.

GWB during the post-monsoon season (Figure 5(c)), which is statistically significant. In winter, the trends weakened again and inclined only to the northeastern GWB (Figure 5(d)). On the other hand, the western and southwestern GWB showed a continuous decreasing pattern during the pre-monsoon (0.001 to −0.006 °C year^{-1}), winter (0.002 to −0.003 °C year^{-1}), and annual (0.006 to −0.001 °C year^{-1}) scales. The monsoon had a neutral trend, whereas the post-monsoon season revealed a rising pattern with less amplitude (0.003–0.008 °C year^{-1}). It seems that the rising pattern of the T_{min} trend gradually faded from pre-monsoon to winter seasons and produced an overall or summative picture of seasonal trends in the annual series.

Irrespective of the seasonal and annual scales, the spatial pattern of P_{rc} in West Bengal showed quite heterogeneous characteristics (Figure 6). Few areas of the SHWB region (especially the Darjeeling Himalaya) witnessed a significant rising pattern consistently in all the seasons, including the annual scale. On the other hand, the north and northeastern Jalpaiguri district, including the eastern Dakshin Dinajpur district from the same region, showed a consistent decrease in P_{rc}, however, significant only on monsoon and annual scales. Both the highest and lowest increase (decrease) were 20.973 (−14.565) and 0.446 (−0.235) mm year^{-1} observed in the annual and winter series, respectively. The increasing trends were mainly prevalent in the western (southern Birbhum, western Bankura, western Burdwan, and eastern Purulia districts) and southwestern GWB (southern and southwestern West and East Medinipur districts) throughout the seasonal and annual levels (except for the post-monsoon season). The post-monsoon season also displayed a rising pattern, but only in the central and southeastern GWB, which comprised southern Nadia, Hugli, Kolkata, Howrah, northern East Medinipur, North 24 Parganas, and the majority of South 24 Parganas districts (Figure 6(c)). The only contrasting feature was that the pre-monsoon, monsoon, and annual time series showed a significantly rising trend, whereas the post-monsoon and winter seasons did not reveal any statistical significance.

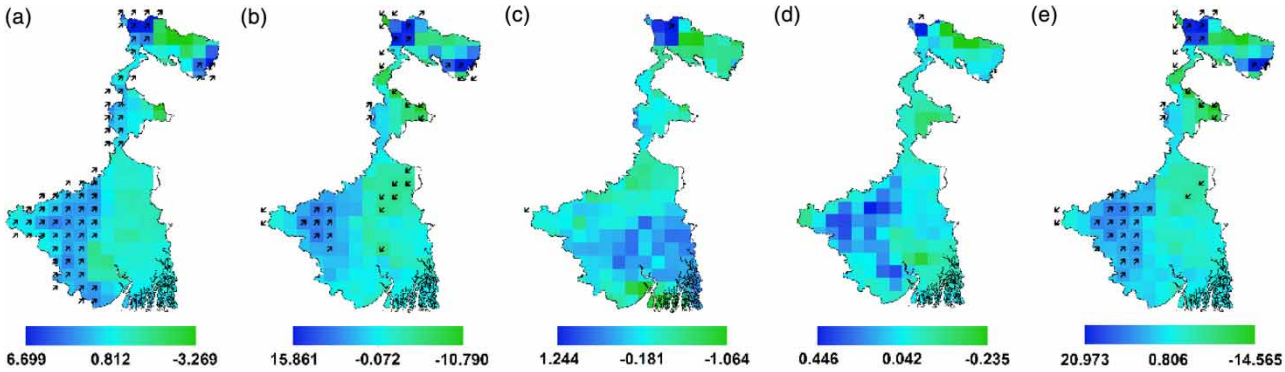

Figure 6 | Rainfall trend and magnitude (mm year^{-1}) during (a) pre-monsoon, (b) monsoon, (c) post-monsoon, (d) winter, and (e) annual scale in West Bengal from 1951 to 2020. The tilted upward arrows indicate significant ($\alpha = 0.05$) increasing trend and *vice versa*.

In general, the ET_0 has decreased in most regions of West Bengal across seasonal and annual scales (Figure 7). While ET_0 fell continuously throughout West Bengal during the pre-monsoon season (Figure 7(a)) at a rate of −0.823 to −0.091 mm year^{-1}, it climbed consistently throughout the monsoon season (Figure 7(b)) at an amplitude of 0.092–0.479 mm year^{-1}. Both the post-monsoon and winter seasons showed a rising and declining trend, respectively (Figure 7(c) and 7(d)). While examining the annual ET_0 trend (Figure 7(e)), we found a non-significant increasing trend in the entire SHWB region and southwestern sections of GWB, including coastline areas. On the other hand, the eastern, western, and central parts of the GWB region exhibited a significant reduction at a rate of −0.245 to −0.904 mm year^{-1}. The maximum rise (fall) and minimum rise (fall) in ET_0 were 0.479 (−0.904) and 0.004 (−0.080) mm year^{-1} observed in the monsoon (annual) and winter (post-monsoon) seasons, respectively.

Except for the monsoon, the S_{rd} trends reduced substantially in West Bengal (Figure 8), particularly in the GWB region. The pre-monsoon season witnessed a substantial fall across West Bengal (Figure 8(a)), significant only in the GWB region, barring a few grids on the western and southern sides. Conversely, the monsoon (Figure 8(b)) displayed an altogether different character, exhibiting a rising tendency throughout West Bengal at a rate of 0.002–0.010 MJ m^{-2} day^{-1} year^{-1}. Both the rising and declining trends were detected in the post-monsoon, winter, and annual time series (Figure 8(c)–8(e)). Increasing trends were observed primarily in the foothills of SHWB (Darjeeling, Jalpaiguri, and Cooch Behar districts), while decreasing trends were prevalent in southern SHWB (Malda and Dakshin Dinajpur districts) as well as in the GWB region, except for a few grids located in the western and southwestern parts that too are only on winter and annual scales. Only a few grids revealed significant rising trends in the western and southwestern GWB during monsoon (Figure 8(b)) and the northeastern portions of the SHWB region during post-monsoon (Figure 8(c)). On the other hand, the annual series revealed no statistical significance

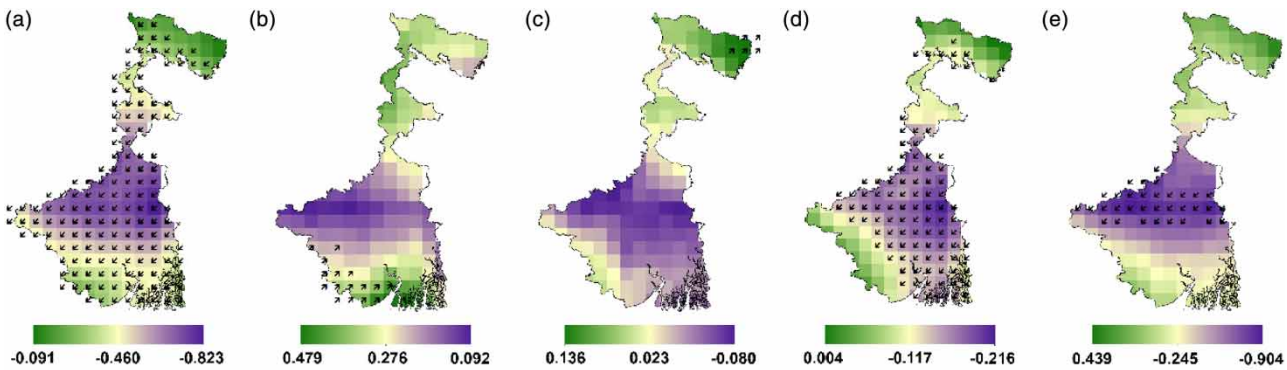

Figure 7 | Spatial pattern of reference evapotranspiration trend and magnitude (mm year^{-1}) during (a) pre-monsoon, (b) monsoon, (c) post-monsoon, (d) winter, and (e) annual scale in West Bengal from 1951 to 2020. The tilted upward arrows indicate significant ($\alpha = 0.05$) increasing trend and *vice versa*.

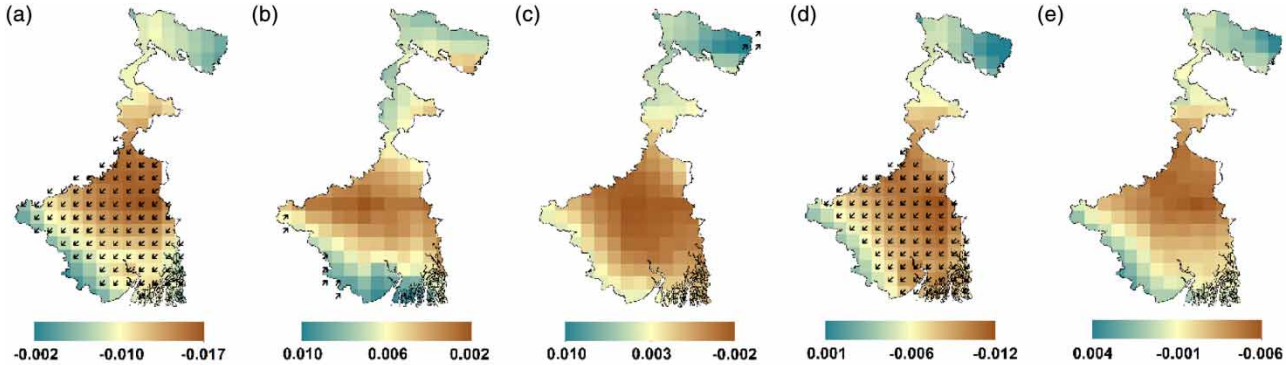

Figure 8 | Spatial trend and magnitude in solar radiation (MJ m^{-2} day^{-1} $year^{-1}$) during (a) pre-monsoon, (b) monsoon, (c) post-monsoon, (d) winter, and (e) annual scale in West Bengal from 1951 to 2020. The tilted upward arrows indicate significant ($\alpha = 0.05$) increasing trend and *vice versa*.

at all (Figure 8(e)). The highest increase (decrease) and lowest increase (decrease) were 0.010 (−0.017) and 0.001 (−0.002) MJ m^{-2} day^{-1} $year^{-1}$ observed in the monsoon (pre-monsoon) and winter (post-monsoon) seasons, respectively.

4. DISCUSSION

Overall, the study found a higher variability of climate dynamics in GWB (particularly in the western and southwestern parts) than in the SHWB region. However, several grids in the north and northeastern SHWB showed higher climate dynamics during pre-monsoon and winter seasons. It is due to the pronounced variability of T_{max} (more than 1.540), S_{rd} (more than 1.300), and ET_0 (more than 1.390). It was further accentuated by the clear-sky conditions during this season because more solar radiation reached the Earth's surface, increasing the energy availability and enhancing the rate of ET_0, eventually exacerbating the variability of climate dynamics. Such a finding was also observed in northern China (Xu *et al.* 2017).

While comparing the results of the present study with those from earlier studies, we found substantial (little) differences considering the variability (trend) of studied climatic parameters, respectively. Except for ET_0, the observed variability and trend of the studied parameters are comparable to previous studies (Mandal *et al.* 2013; Sharma *et al.* 2016; Datta & Das 2019a, 2022) for the SHWB region (barring a few areas in Cooch Behar and Jalpaiguri districts) while contrasting for the GWB region (particularly in the western, southwestern, and central parts). Broadly, the ET_0 trend corresponds to the findings of Bandyopadhyay *et al.* (2009) for the GWB region (except for monsoon and post-monsoon) and contradicts the outcomes of Jhajharia *et al.* (2012) for the SHWB region (except for pre-monsoon and winter). Such disparities might be attributed to the differential analysis period and timescales to construct seasonal data (like January–February vs. December–January–February for winter), including the preferred methodologies. Notably, regions with higher variability in previous studies usually exhibited a lower variability in the present study and *vice versa*. For instance, Sadhukhan *et al.* (2000) reported a higher rainfall variability in the central and northwestern GWB region during the pre-monsoon season, whereas the present study observed a lower variability. Likewise, Datta & Das (2019b) found a rising T_{max} and T_{min} variability in the Darjeeling and Malda districts within the SHWB region, but the current study revealed declining variability (barring a few grids in Darjeeling during pre-monsoon and winter seasons) as the fractal dimension of those areas ranges between 1.276 and 1.334 compared to the higher variability areas of 1.472–1.545 (Supplementary Figures S1 and S2). It is likely to use fractal dimension, which provides more detailed characteristics across space and time than the conventional coefficient of variation technique often used in earlier studies. Moreover, regions with higher variability of climate dynamics appeared to have unclear long-term trends, making them highly unpredictable.

Since the GWB is one of India's crucial rice-growing belts, higher variability of climate dynamics across seasonal and annual scales could have far-reaching consequences on agricultural production. Furthermore, temperature rises in this region are expected to impact crop growth by increasing respiration and basal metabolism and modifying the plant response system to various biotic stresses. On the other hand, declining monsoonal rainfall coupled with rising ET_0 may result in reduced water and soil moisture availability, followed by drought. Together, these changes will negatively impact agricultural production, especially rice productivity, by lowering the biomass and yield. Since more than 6% of India's food production

exclusively comes from West Bengal (Government of India 2018b), such a situation is alarming for the livelihood of the booming population and the country's ability to feed itself. Apart from this, higher variability of climate dynamics means more complexity and uncertainty, which may inhibit farmers' decision-making regarding principal food grain (especially rice) production, as they will not be able to anticipate the changes in the onset and cessation of monsoon, occurrence of consecutive dry and wet spells, and so on. Inevitably, the farmers of this region rely on irrigation facilities to meet the crop water demand even in monsoon months, leading to 31 m of groundwater level depletion, as found by Pradhan *et al.* (2022). The uncertain climate and plummeting groundwater levels could force farmers to switch to less water-intensive non-food grain production, such as oilseeds, sugarcane, and mesta, despite those crops requiring longer growing days. Such evidence has already been observed in several districts of West Bengal. For instance, the non-food crop acreage has increased (from 2004–05 to 2014–15) in Bankura, Burdwan, Cooch Behar, and Purulia districts, albeit marginally (Government of West Bengal 2016).

The present study also reveals a moderate variability (4.209–4.619) of climate dynamics in the SHWB region, notably in a few isolated areas of Darjeeling, Jalpaiguri, and Cooch Behar districts during the lean period (October–May). A further variation in climate dynamics, including rising temperature, evapotranspiration, and diminishing rainfall, may increase the likelihood of drought, impacting the world-renowned Darjeeling tea production. Surprisingly, this region, which used to be abundant in groundwater, has also shown diminution in recent decades due to over-abstraction followed by decreasing rainfall (Rudra 2017). Therefore, there is a need for efficient crop and water management not only to offset any further deterioration of groundwater but also to reduce crops' vulnerability and risk from climate change and/or variability. In this regard, agroforestry, short-duration cultivars, crop rotation and diversification, and mixed farming could be viable options concerning crop management. For groundwater depletion, using deep farm ponds might lessen the risk while restoring soil moisture and providing irrigation to fulfill crop water needs during dry seasons (Das *et al.* 2022). Additionally, encouraging maize over water-intensive Boro rice during the Rabi season (October–May) may revive groundwater levels as it only requires one-fifth of the total water consumed by rice and delivers higher returns (Kapuria & Banerjee 2022). On the other hand, the foothills of the SHWB have significant potential for mushroom farming (Datta & Das 2021), which may also be adopted to minimize the additive economic damages.

5. CONCLUSION AND THE WAY FORWARD

The present study examined the spatio-temporal variability of climate dynamics by integrating five climatic parameters (T_{max}, T_{min}, P_{rc}, ET_0, and S_{rd}) critical for field-crop production through the lens of fractal dimensions over the Indian state of West Bengal from 1951 to 2020. Furthermore, this study assessed the trend and magnitudes of those climatic parameters to comprehend the changing climate scenarios holistically. The results showed a higher variability of climate dynamics in the western, southern, and southwestern GWB, whereas central, eastern, and southeastern sections showed a modest degree of variability with an increasing trend in temperature and a decreasing trend in rainfall. Contrarily, the SHWB witnessed a lower fractal dimension in all parameters, resulting in low variability. Nevertheless, the immediate foothill areas of SHWB (especially Darjeeling, Jalpaiguri, and Cooch Behar districts) exhibited a modest degree of variation in climate dynamics along with a rising trend in temperatures and reference evapotranspiration and a decreasing trend in rainfall during the post-monsoon and winter seasons, indicating the possibility of drought in the near future. Furthermore, the study observed the presence of persistence, anti-persistence, neutral, and self-similar patterns among the analyzed variables. However, more research is required to untangle such a complex behavior of climatic factors, which would contribute to a more comprehensive understanding of the changing climate dynamics. Considering variability, trend, and magnitudes of the analyzed parameters, the study identified (i) the western and southwestern GWB; (ii) the coastal belts, especially the deltaic areas of the Sundarbans; and (iii) the immediate foothills of the SHWB region as the climatically most vulnerable areas in West Bengal and in need of proactive crop and water management policy measures.

The changing climate has significant repercussions on agricultural productivity, followed by food security, livelihoods, and socio-economic development of the growing human population. A marginal increase in the non-food crop area signifies a short-term adjustment or business-as-usual strategy to offset the economic loss due to the yield reduction in conventional food grain production under highly complex and uncertain climatic conditions. A low to moderate crop diversification rate in the GWB region, specifically in Purulia, Bankura, Birbhum, and Burdwan districts (Birthal & Hazrana 2019), corroborated our standpoint. Indeed, such an adjustment in crop cultivation solely driven by profit maximizations under climate

change may have helped the farmers achieve some economic stability; however, it might not be a sustainable path considering the global issue of food security. Sustainable food security requires systemic and transformational change (Campbell *et al.* 2018; Vermeulen *et al.* 2018) in a feasible manner, i.e., strategies with values and visions and the way they are implemented in practice (Bentz *et al.* 2022), which is currently lacking in the state (for instance, see Dey *et al.* 2016). Therefore, future studies should include crucial socio-politico-economic attributes to examine how climate dynamics, including climate-induced extremes, affect the agricultural systems and render them susceptible, which may aid in formulating appropriate adaptation strategies.

ACKNOWLEDGEMENTS

The authors express their gratitude to the Editor-in-Chief, the Associate Editor, and the anonymous reviewers for their critical review and constructive suggestions. The first author received support from the University Grants Commission (UGC), New Delhi, India, in the form of the Junior (Senior) Research Fellowship Award [(Award No. 3291/(SC)(NET-DEC.2015)] to pursue the research. Furthermore, the first author would like to thank Lilu Bhoi for his assistance in coding and Pritha Datta for her encouragement and insightful input on the study design.

AUTHOR CONTRIBUTIONS

S.D. worked on conceptualization, formal analysis, methodology, resources, software, visualization, writing – original draft, writing – review and editing. K.G. focused on conceptualization, supervision, validation, writing – review and editing.

FUNDING

The authors declare that the article is not funded by any scientific institution.

DATA AVAILABILITY STATEMENT

All relevant data are included in the paper or its Supplementary Information.

CONFLICT OF INTEREST

The authors declare there is no conflict.

REFERENCES

Allen, R. G., Pereira, L. S., Raes, D. & Smith, M. 1998 *Crop Evapotranspiration – Guidelines for Computing Crop Water Requirements*. FAO Irrigation and Drainage, Paper No. 56. FAO, Rome, Vol. 300, No. 9, p. D05109.

Bandyopadhyay, A., Bhadra, A., Raghuwanshi, N. S. & Singh, R. 2009 Temporal trends in estimates of reference evapotranspiration over India. *Journal of Hydrologic Engineering* **14** (5), 508–515. https://doi.org/10.1061/(ASCE)HE.1943-5584.0000006.

Basha, G., Kishore, P., Ratnam, M. V., Jayaraman, A., Kouchak, A. A., Ouarda, T. B. & Velicogna, I. 2017 Historical and projected surface temperature over India during the 20th and 21st century. *Scientific Reports* **7**, 2987. https://doi.org/10.1038/s41598-017-02130-3.

Bentz, J., O'Brien, K. & Scoville-Simonds, M. 2022 Beyond 'blah blah blah': exploring the 'how' of transformation. *Sustainability Science* **17** (2), 497–506. https://doi.org/10.1007/s11625-022-01123-0.

Birthal, P. S. & Hazrana, J. 2019 Crop diversification and resilience of agriculture to climatic shocks: evidence from India. *Agricultural Systems* **173**, 345–354. https://doi.org/10.1016/j.agsy.2019.03.005.

Boyd, E. 2017 Climate adaptation: holistic thinking beyond technology. *Nature Climate Change* **7**, 97–98. https://doi.org/10.1038/nclimate3211.

Campbell, B. M., Hansen, J., Rioux, J., Stirling, C. M. & Twomlow, S. 2018 Urgent action to combat climate change and its impacts (SDG 13): transforming agriculture and food systems. *Current Opinion in Environmental Sustainability* **34**, 13–20. https://doi.org/10.1016/j.cosust.2018.06.005.

Census of India. 2011 District Census Handbook (DCHB) of West Bengal. Available from: www.censusindia.gov.in/2011census/dchb/WBA.html (accessed 25 May 2019).

Cline, W. R. 2008 Global warming and agriculture. *Finance & Development* **45** (1), 23–27.

Cui, B., Huang, P. & Xie, W. 2022 Fractal dimension characteristics of wind speed time series under typhoon climate. *Journal of Wind Engineering and Industrial Aerodynamics* **229**, 105144. https://doi.org/10.1016/j.jweia.2022.105144.

Das, S. & Goswami, K. 2021 Progress in agricultural vulnerability and risk research in India: a systematic review. *Regional Environmental Change* **21** (24), 1–18. https://doi.org/10.1007/s10113-021-01749-3.

Das, S., Datta, P., Sharma, D. & Goswami, K. 2022 Trends in temperature, precipitation, potential evapotranspiration, and water availability across the Teesta River Basin under 1.5 and 2° C temperature rise scenarios of CMIP6. *Atmosphere* **13** (6), 941. https://doi.org/10.3390/atmos13060941.

Dash, S. K., Jenamani, R. K., Kalsi, S. R. & Panda, S. K. 2007 Some evidence of climate change in twentieth-century India. *Climatic Change* **85** (3–4), 299–321. https://doi.org/10.1007/s10584-007-9305-9.

Datta, P. & Das, S. 2019a Analysis of long-term precipitation changes in West Bengal, India: an approach to detect monotonic trends influenced by autocorrelations. *Dynamics of Atmospheres and Oceans* **88**, 101118. https://doi.org/10.1016/j.dynatmoce.2019.101118.

Datta, P. & Das, S. 2019b Analysis of long-term seasonal and annual temperature trends in North Bengal, India. *Spatial Information Research* **27** (4), 475–496. https://doi.org/10.1007/s41324-019-00250-8.

Datta, P. & Das, S. 2021 Model-based strategic planning for strengthening mushroom entrepreneurship: insights from a sub-Himalayan region of West Bengal, India. *GeoJournal* **86** (1), 145–158. https://doi.org/10.1007/s10708-019-10063-9.

Datta, P. & Das, S. 2022 Assessing the consistency of trends in Indian summer monsoon rainfall. *Hydrological Sciences Journal* **67** (9), 1384–1396. https://doi.org/10.1080/02626667.2022.2081507.

Dey, S., Ghosh, A. K. & Hazra, S. 2016 Review of West Bengal State Adaptation Policies, Indian Bengal Delta. DECCMA Working Paper, Deltas, Vulnerability and Climate Change: Migration and Adaptation, IDRC Project Number 107642. Available from: http://generic.wordpress.soton.ac.uk/deccma/resources/working-papers/ (accessed 10 July 2022).

Feder, J. 1988 *Fractals*. 1st edn. Springer, New York.

Fortuna, L., Nunnari, S. & Guariso, G. 2014 Fractal order evidences in wind speed time series. In *Proceedings of the ICFDA'14 International Conference on Fractional Differentiation and Its Applications 2014*, 23–25 June 2014, Catania, Italy. IEEE, pp. 1–6. https://doi.org/10.1109/ICFDA.2014.6967450.

Government of India. 2018a *Economic Survey – 2018: Climate, Climate Change, and Agriculture*. Department of Economic Affairs, Ministry of Finance, Government of India, New Delhi. Available from: https://www.im4change.org/docs/740economic%20survey%202017-18%20-%20vol.I.pdf (accessed 10 October 2023).

Government of India. 2018b *Pocket Book of Agricultural Statistics 2017*. Directorate of Economics & Statistics, Department of Agriculture, Cooperation & Farmers Welfare, Ministry of Agriculture & Farmers Welfare, New Delhi. Available from: https://agricoop.nic.in/sites/default/files/pocketbook_0.pdf (accessed 9 January 2022).

Government of West Bengal. 2010 *Economic Review of West Bengal 2009-10*. Bureau of Applied Economics & Statistics, Development & Planning Department, Government of West Bengal, Kolkata.

Government of West Bengal. 2016 *State Statistical Handbook West Bengal 2015*. Bureau of Applied Economics & Statistics, Development & Planning Department, Kolkata. Available from: http://www.wbpspm.gov.in/SiteFiles/Publications/3_18052017140119.pdf (accessed 17 May 2020).

Hamed, K. H. & Rao, A. R. 1998 A modified Mann-Kendall trend test for autocorrelated data. *Journal of Hydrology* **204** (1–4), 182–196. https://doi.org/10.1016/S0022-1694(97)00125-X.

Hargreaves, G. H. & Samani, Z. A. 1985 Reference crop evapotranspiration from temperature. *Applied Engineering in Agriculture* **1** (2), 96–99. https://doi.org/10.13031/2013.26773.

Harrouni, S. & Guessoum, A. 2009 Using fractal dimension to quantify long-range persistence in global solar radiation. *Chaos, Solitons & Fractals* **41** (3), 1520–1530. https://doi.org/10.1016/j.chaos.2008.06.016.

Hersbach, H., Bell, B., Berrisford, P., Hirahara, S., Horányi, A., Muñoz-Sabater, J., Nicolas, J., Peubey, C., Radu, R., Schepers, D. & Simmons, A. 2020 The ERA5 global reanalysis. *Quarterly Journal of the Royal Meteorological Society* **146** (730), 1999–2049. https://doi.org/10.1002/qj.3803.

Hurst, H. E. 1951 Long-term storage capacity of reservoirs. *Transactions of the American Society of Civil Engineers* **116**, 770–808. https://doi.org/10.1061/TACEAT.0006518.

IMD. 2008 *Climate of West Bengal*. Controller of Publications, National Climate Center, Additional Director General of the Meteorology (Research), India Meteorological Department, Pune, India.

Jabal, Z. K., Khayyun, T. S. & Alwan, I. A. 2022 Impact of climate change on crops productivity using MODIS-NDVI time series. *Civil Engineering Journal* **8** (6). https://doi.org/10.28991/CEJ-2022-08-06-04.

Jhajharia, D., Dinpashoh, Y., Kahya, E., Singh, V. P. & Fakheri-Fard, A. 2012 Trends in reference evapotranspiration in the humid region of northeast India. *Hydrological Processes* **26** (3), 421–435. https://doi.org/10.1002/hyp.8140.

Kapuria, P. & Banerjee, S. 2022 *Crop Shifting for Improved Water Use and Nutritional Productivity in the Lower Indo-Gangetic Plains of West Bengal*. ORF Occasional Paper No. 358, June 2022, Observer Research Foundation.

Kendall, M. G. 1975 *Rank Correlation Methods*. Charles Griffen, London.

Kim, J. & Ivanov, V. Y. 2015 A holistic, multi-scale dynamic downscaling framework for climate impact assessments and challenges of addressing finer-scale watershed dynamics. *Journal of Hydrology* **522**, 645–660. https://doi.org/10.1016/j.jhydrol.2015.01.025.

Mahto, S. S. & Mishra, V. 2019 Does ERA-5 outperform other reanalysis products for hydrologic applications in India? *Journal of Geophysical Research: Atmospheres* **124** (16), 9423–9441. https://doi.org/10.1029/2019JD031155.

Mandal, S., Choudhury, B. U., Mondal, M. & Bej, S. 2013 Trend analysis of weather variables in Sagar Island, West Bengal, India: a long-term perspective (1982–2010). *Current Science* **105** (7), 947–953. Available from: https://www.jstor.org/stable/24098514.

Mandelbrot, B. B. & Wallis, J. R. 1969 Computer experiments with fractional Gaussian noises: part 3, mathematical appendix. *Water Resources Research* **5** (1), 260–267. https://doi.org/10.1029/WR005i001p00260.

Mann, H. B. 1945 Non-parametric tests against trend. *Econometrica: Journal of Econometric Society* **13** (3), 245–259. https://doi.org/10.2307/1907187.

Mann, R. & Gupta, A. 2022 Temporal trends of rainfall and temperature over two sub-divisions of Western Ghats. *HighTech and Innovation Journal* **3**, 28–42. https://doi.org/10.28991/HIJ-SP2022-03-03.

MOSPI. 2021 Sector-wise GDP of India. Available from: https://statisticstimes.com/economy/country/india-gdp-sectorwise.php (accessed 21 August 2022).

Mukhopadhyay, S., Kulkarni, S., Kulkarni, P. & Dutta, S., 2016 Rainfall statistics change in West Bengal (India) from period 1901-2000. In: *Geostatistical and Geospatial Approaches for the Characterization of Natural Resources in the Environment* (Raju, N., ed.). Springer, Cham, pp. 173–181.

Pai, D. S., Rajeevan, M., Sreejith, O. P., Mukhopadhyay, B. & Satbha, N. S. 2014 Development of a new high spatial resolution (0.25 × 0.25) long period (1901–2010) daily gridded rainfall data set over India and its comparison with existing data sets over the region. *Mausam* **65** (1), 1–18. https://doi.org/10.54302/mausam.v65i1.851.

Parry, M. L., Rosenzweig, C., Iglesias, A., Livermore, M. & Fischer, G. 2004 Effects of climate change on global food production under SRES emissions and socio-economic scenarios. *Global Environmental Change* **14** (1), 53–67. https://doi.org/10.1016/j.gloenvcha.2003.10.008.

Peel, M. C., Finlayson, B. L. & McMahon, T. A. 2007 Updated world map of the Köppen-Geiger climate classification. *Hydrology and Earth System Sciences* **11** (5), 1633–1644. https://doi.org/10.5194/hess-11-1633-2007.

Pradhan, S., Dhar, A. & Tiwari, K. N. 2022 Sustainability of Boro rice cultivation in the canal irrigated command area of India. *Journal of Water and Climate Change*, jwc2022125. https://doi.org/10.2166/wcc.2022.125.

Ramanathan, V., Ramana, M. V., Roberts, G., Kim, D., Corrigan, C., Chung, C. & Winker, D. 2007 Warming trends in Asia amplified by brown cloud solar absorption. *Nature* **448** (7153), 575–578.

Rangarajan, G. & Sant, D. A. 2004 Fractal dimensional analysis of Indian climatic dynamics. *Chaos, Solitons & Fractals* **19** (2), 285–291. https://doi.org/10.1016/S0960-0779(03)00042-0.

Rao, B. B., Chowdary, P. S., Sandeep, V. M., Rao, V. U. M. & Venkateswarlu, B. 2014 Rising minimum temperature trends over India in recent decades: implications for agricultural production. *Global and Planetary Change* **117**, 1–8. https://doi.org/10.1016/j.gloplacha.2014.03.001.

Rao, B. B., Chowdary, P. S., Sandeep, V. M., Pramod, V. P. & Rao, V. U. M. 2015 Spatial analysis of the sensitivity of wheat yields to temperature in India. *Agricultural and Forest Meteorology* **200**, 192–202. https://doi.org/10.1016/j.agrformet.2014.09.023.

Rathore, L. S., Attri, S. D. & Jaswal, A. K. 2013 *State Level Climate Change Trends in India. Meteorological Monograph No. ESSO/IMD/EMRC/02/2013*. India Meteorological Department, Ministry of Earth Sciences, New Delhi.

Rind, D. 1999 Complexity and climate. *Science* **284** (5411), 105–107. https://doi.org/10.1126/science.284.5411.105.

Rudra, K., 2017 Sharing water across Indo-Bangladesh border. In: *Regional Cooperation in South Asia* (Bandyopadhyay, S., Torre, A., Casaca, P. & Dentinho, T., eds). Contemporary South Asian Studies. Springer, Cham, pp. 189–207.

Sadhukhan, I., Lohar, D. & Pal, D. K. 2000 Pre-monsoon season rainfall variability over Gangetic West Bengal and its neighbourhood, India. *International Journal of Climatology* **20** (12), 1485–1493. https://doi.org/10.1002/1097-0088(200010)20:12%3C1485::AID-JOC544%3E3.0.CO;2-V.

Sen, P. K. 1968 Estimates of the regression coefficient based on Kendall's tau. *Journal of the American Statistical Association* **63** (324), 1379–1389. https://doi.org/10.1080/01621459.1968.10480934.

Sharma, C. S., Panda, S. N., Pradhan, R. P., Singh, A. & Kawamura, A. 2016 Precipitation and temperature changes in eastern India by multiple trend detection methods. *Atmospheric Research* **180**, 211–225. https://doi.org/10.1016/j.atmosres.2016.04.019.

Singh, D., Tsiang, M., Rajaratnam, B. & Diffenbaugh, N. S. 2014 Observed changes in extreme wet and dry spells during the South Asian summer monsoon season. *Nature Climate Change* **4**, 456–461. https://doi.org/10.1038/nclimate2208.

Sonali, P. & Kumar, D. N. 2013 Review of trend detection methods and their application to detect temperature changes in India. *Journal of Hydrology* **476**, 212–227. https://doi.org/10.1016/j.jhydrol.2012.10.034.

Srivastava, A. K., Rajeevan, M. & Kshirsagar, S. R. 2009 Development of a high resolution daily gridded temperature data set (1969–2005) for the Indian region. *Atmospheric Science Letters* **10** (4), 249–254. https://doi.org/10.1002/asl.232.

Srivastava, P., Singh, R., Tripathi, S. & Raghubanshi, A. S. 2016 An urgent need for sustainable thinking in agriculture – an Indian scenario. *Ecological Indicators* **67**, 611–622. https://doi.org/10.1016/j.ecolind.2016.03.015.

Vermeulen, S. J., Dinesh, D., Howden, S. M., Cramer, L. & Thornton, P. K. 2018 Transformation in practice: a review of empirical cases of transformational adaptation in agriculture under climate change. *Frontiers in Sustainable Food Systems* **2** (65), 1–17. https://doi.org/10.3389/fsufs.2018.00065.

Xu, J., Chen, Y., Li, W., Liu, Z., Tang, J. & Wei, C. 2016 Understanding temporal and spatial complexity of precipitation distribution in Xinjiang, China. *Theoretical and Applied Climatology* **123** (1), 321–333. https://doi.org/10.1007/s00704-014-1364-z.

Xu, Z., Tang, Y., Connor, T., Li, D., Li, Y. & Liu, J. 2017 Climate variability and trends at a national scale. *Scientific Reports* **7**, 3258. https://doi.org/10.1038/s41598-017-03297-5.

First received 29 April 2023; accepted in revised form 20 September 2023. Available online 4 October 2023